ISSN 1674-1056
http://cpb.iphy.ac.cn
http://iopscience.iop.org/cpb
中国物理 B
Chinese Physics
中国物理 Chinese Physics B

Phase-related noise characteristics of 780 nm band single-frequency lasers used in the cold atomic clock

Xi Zhang(张茜), Fei Yang(杨飞), Zi-Tong Feng(冯子桐), Jie-Jun Zhao(赵洁珺), Fang Wei(魏芳), Hai-Wen Cai(蔡海文), Rong-Hui Qu(瞿荣辉)

Citation: Chin. Phys. B . 2019, 28(7): 074209. **doi:** 10.1088/1674-1056/28/7/074209
Journal homepage: http://cpb.iphy.ac.cn; http://iopscience.iop.org/cpb

What follows is a list of articles you may be interested in

High-power and high optical conversion efficiency diode-end-pumped laser with multi-segmented Nd: YAG/Nd: YVO_4

Meng-Yao Wu(吴梦瑶), Peng-Fei Qu(屈鹏飞), Shi-Yu Wang(王石语), Zhen Guo(过振), De-Fang Cai(蔡德芳), Bing-Bin Li(李兵斌)
Chin. Phys. B . 2018, 27(9): 094207. **doi:** 10.1088/1674-1056/27/9/094207

Tunable Nd, La: SrF_2 laser and passively Q-switched operation based on gold nanobipyramids saturable absorber

Feng Zhang(张峰), Hua-Nian Zhang(张华年), Dan-Hua Liu(刘丹华), Jie Liu(刘杰), Feng-Kai Ma(马凤凯), Da-Peng Jiang(姜大朋), Si-Yuan Pang(逄思远), Liang-Bi Su(苏良碧), Jun Xu(徐军)
Chin. Phys. B . 2017, 26(2): 024205. **doi:** 10.1088/1674-1056/26/2/024205

An efficient continuous-wave YVO_4/Nd: YVO_4/YVO_4 self-Raman laser pumped by a wavelength-locked 878.9 nm laser diode

Li Fan(樊莉), Weiqian Zhao(赵伟倩), Xin Qiao(乔鑫), Changquan Xia(夏长权), Lichun Wang(汪丽春), Huibo Fan(范会博), Mingya Shen(沈明亚)
Chin. Phys. B . 2016, 25(11): 114207. **doi:** 10.1088/1674-1056/25/11/114207

High-energy femtosecond Yb-doped all-fiber monolithic chirped-pulse amplifier at repetition rate of 1 MHz

Zhi-Guo Lv(吕志国), Hao Teng(滕浩), Li-Na Wang(王立娜), Jun-Li Wang(王军利), Zhi-Yi Wei(魏志义)
Chin. Phys. B . 2016, 25(9): 094208. **doi:** 10.1088/1674-1056/25/9/094208

Generation of 15 W femtosecond laser pulse from a Kerr-lens mode-locked Yb: YAG thin-disk oscillator

Yingnan Peng(彭英楠), Jinwei Zhang(张金伟), Zhaohua Wang(王兆华), Jiangfeng Zhu(朱江峰), Dehua Li(李德华), Zhiyi Wei(魏志义)
Chin. Phys. B . 2016, 25(9): 094207. **doi:** 10.1088/1674-1056/25/9/094207

Phase-related noise characteristics of 780 nm band single-frequency lasers used in the cold atomic clock*

Xi Zhang(张茜)[1,2], Fei Yang(杨飞)[1,†], Zi-Tong Feng(冯子桐)[1,2], Jie-Jun Zhao(赵洁珺)[1,2], Fang Wei(魏芳)[1], Hai-Wen Cai(蔡海文)[1,2,‡], and Rong-Hui Qu(瞿荣辉)[1]

[1] *Key Laboratory of Space Laser Communication and Detection Technology, Shanghai Institute of Optics and Fine Mechanics, Chinese Academy of Sciences, Shanghai* 201800, *China*

[2] *Center of Materials Science and Optoelectronics Engineering, University of Chinese Academy of Sciences, Beijing* 100049, *China*

(Received 8 April 2019; revised manuscript received 9 May 2019; published online 12 June 2019)

We propose a method to directly measure phase-related noise characteristics of single-frequency lasers in the 728–980 nm band based on a 120° phase difference interferometer. Differential phase information of the laser under test is demodulated via the interferometer. Other parameters related to the phase noise characteristics such as linewidth at different observation time, phase/frequency noise, power spectrum density of phase/frequency fluctuation, and Allan deviation are further obtained. Frequency noise as low as 1 Hz^2/Hz can be measured using our system. Then the phase-related noise characteristics of two commercial lasers frequently used in cold atomic clocks are studied systematically by the method. Furthermore, several influencing factors and their relative evolution laws are also revealed, such as the pump current and frequency-locking control parameters. This would help to optimize the laser performance, select laser sources, and evaluate the system performance for cold atomic physics applications.

Keywords: cold atomic physics, quantum mechanics, 780 nm lasers, phase/frequency noise

PACS: 42.55.–f, 42.60.Mi, 31.30.J–, 03.75.Be **DOI:** 10.1088/1674-1056/28/7/074209

1. Introduction

The frequency of 780 nm corresponds to the D2 line of rubidium (Rb) atoms, this implies that the lasers in the 780 nm band are useful in quantum mechanics and atomic physics. For example, they play an important role in pumping Rb atoms in a Rb fountain atomic clock.[1–4] Additionally, it is vital for laser cooling and imprisoning atoms,[5] atomic interferometry,[6] as well as establishing new quantum frequency standards.[7]

Phase-related noise characteristics are essential aspects of laser performance, especially the linewidth parameter. Most atomic physics applications involving atomic fine structure sub-levels, such as Rb fountain atomic clocks, laser cooling and atom imprisoning, and high-resolution spectrum, require laser sources with good phase noise characteristics to pump atoms. Specifically, it is necessary to select laser sources with a linewidth at the MHz scale or below for the purpose of measuring the spectroscopy of the D1 and D2 lines of Rb due to the natural linewidth of the corresponding transition (6 MHz).[5] Several methods for laser phase-related noise characteristics are developed, including optical spectrum analyzers, Fabry–Perot resonators, coherent discrimination detection techniques, and self-delayed heterodyne/homodyne and heterodyne methods.[8–12] But the resolution of the system or the integrity of parameters under test is not high enough to characterize the phase-related noise features of a narrow linewidth single frequency laser. With the development of quantum mechanics and atomic physics, scientists have investigated the fundamental dynamics of lasers with wavelength of 780 nm. In 2015, Xu *et al.* proposed a method based on a 120° phase difference interferometer to investigate the phase-noise characteristics of lasers in the 1550 nm band,[10] which provides a direction for us to further investigate the phase-correlated parameters of lasers in the 780 nm band. But the adaptability improvement of the method for 780 nm band is necessary.

In this paper, we present a robust method based on a 120° phase difference interferometer to directly measure the phase-related noise characteristics of single-frequency lasers in the 780 nm band used in quantum physics and cold atomic physics research. The interferometer determines the differential phase information of the laser, thereby, allowing a more complete characterization of the noise of lasers that are tested. In particular, the linewidth at different integration time and Allan deviation of the laser are subsequently calculated from the frequency fluctuation power spectrum density (PSD). The equipment is used to characterize the phase-related noise of a laser and investigate several influencing factors, such as the pump current and frequency locking.

*Project supported by the National Natural Science Foundation of China (Grant Nos. 61875214, 61535014, and 61775225) and Scientific Innovation Fund of Chinese Academy of Sciences (Grant No. CXJJ-17S010).

†Corresponding author. E-mail: fyang@siom.ac.cn

‡Corresponding author. E-mail: hwcai@siom.ac.cn

© 2019 Chinese Physical Society and IOP Publishing Ltd

2. Experimental setup

The system structure diagram of the measurement setup to investigate the phase-related noise characteristics of single-frequency laser sources in the 780 nm band is shown in Fig. 1. The 120° phase difference interferometer is composed of a 3×3 optical coupler (OC) and two Faraday mirrors (FRMs). The laser under test as an input signal is adjusted to an appropriate power level through an optical power control unit and input to port1 of a circulator (CIR). Then, the light is split into three beams via the OC after exiting from port2 of the CIR that is connected to the input port1 of the OC. Two of the laser beams mutually interfere at the OC with a different time delay of 140.8 ns (the corresponding free spectral range is 7.1 MHz) by using a delay fiber after being reflected by the FRMs. The FRMs effectively suppress polarization fading. The output port2 of the OC is empty. The interference beam is then split into three beams again, which enter port3 of the CIR and the input port2 and port3 of the OC. All the fiber components are designed specially and made of Corning HI780 fiber with large bandwidth and low loss as high as possible in order to obtain the maximum range of light and minimum insertion loss. The CIR has almost 100 nm bandwidth with less than 2 dB insertion loss and higher than 25 dB isolation; the OC has almost 100 nm bandwidth with less than 3.3 dB insertion loss; and the FRM has almost 100 nm bandwidth with less than 1.3 dB insertion loss. Besides, we add an additional high-quality and low-noise optical amplifier to conduct power calibration if the input signal is small, which has no influence on the measurement results according to existing studies.[13] The input signal can be as low as −50 dBm, and the output can be set to 10 dBm in automatic power control mode (APC) for further measurement. The interferometer is packaged in an ambient insulation box with controlled temperature, sound, and vibration. Subsequently, they are detected by three identical detectors and collected by a high-speed acquisition card for analysis. Besides, the entire system is powered by dry batteries for lower noise floor and the power is monitored by a battery monitor unit. An embedded computer system manages the analysis of the acquisition data and loading the calculated results to the cloud. As a result, it is convenient for the users to upload and investigate the relative measurement results.

The phase-related noise parameters of the single-frequency lasers in the 780 nm band are reconstructed via differential phase information demodulated by the 120° phase difference interferometer, which is consistent with extant studies.[10] The differential phase accumulated by the 120° phase difference interferometer at the differential delay time τ is as follows:

$$\Delta\varphi(t)=\varphi(t)-\varphi(t-\tau)=\arctan\left(\frac{X_2'(t)}{X_1'(t)}\right)-\overline{\arctan\left(\frac{X_2'(t)}{X_1'(t)}\right)},$$

where $\varphi(t)$ denotes the instantaneous phase of the laser that is to be tested at time t, and $X_1'(t)$ and $X_2'(t)$ are expressed as follows:

$$\begin{pmatrix}X_1'(t)\\X_2'(t)\\X_3'(t)\end{pmatrix}=\begin{pmatrix}\eta_1&\varsigma_1&\xi_1\\\eta_2&\varsigma_2&\xi_2\\\eta_3&\varsigma_3&\xi_3\end{pmatrix}^{-1}\begin{pmatrix}I_1(t)\\I_2(t)\\I_3(t)\end{pmatrix},$$

where $I_n(t)$ $(n=1,2,3)$ denotes the output electrical current of the interferometer with a 120° phase difference, and the parameters η_n, ζ_n, and ξ_n denote constants for the setup. Subsequently, the differential phase PSD of the laser, $S_{\Delta\varphi}(f)$, is calculated from the differential phase information. The other parameters related with the phase-related noise of the lasers are

$$S_\varphi(f)=\frac{1}{4\left(\sin(\pi f\tau)\right)^2}S_{\Delta\varphi}(f)=2L(f),$$

$$S_\nu(f)=\frac{f^2}{4\left(\sin(\pi f\tau)\right)^2}S_{\Delta\varphi}(f)=\frac{1}{\left(\sin c(\pi f\tau)\right)^2}S_{\Delta\nu}(f),$$

$$\sigma_y(\tau)=\left[\frac{2}{\nu_0^2}\int_0^{f_h}S_\nu(f)\frac{\sin^4(\pi f\tau)}{(\pi f\tau)^2}\mathrm{d}f\right]^{1/2},$$

where $S_\varphi(f)$ denotes the phase noise PSD, $L(f)$ denotes the single-sideband phase noise PSD, $S_{\Delta\nu}(f)$ denotes the differential frequency noise PSD, $S_\nu(f)$ denotes the frequency noise PSD, $\sigma_y(\tau)$ denotes the Allan deviation,[14] and f_h denotes the integral upper limit frequency.

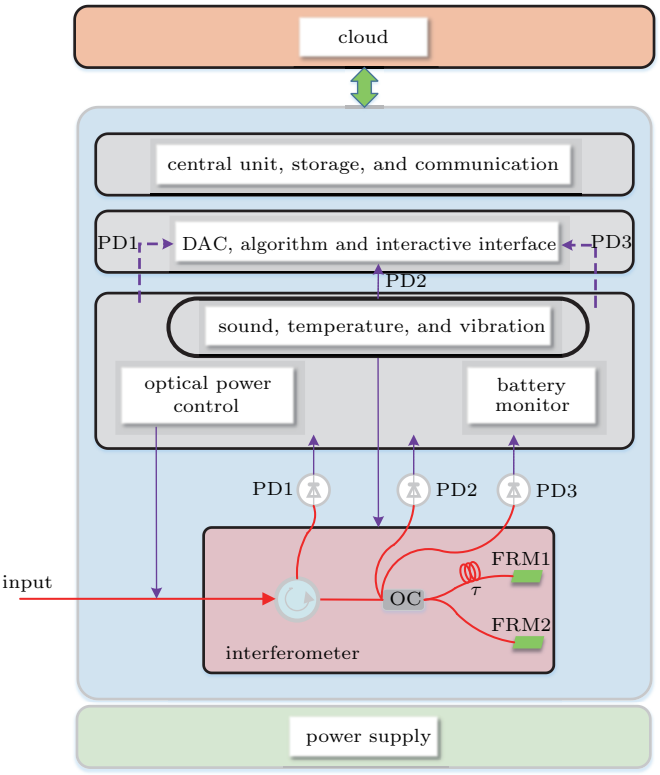


Fig. 1. Structure diagram of the measurement setup. OC, optical coupler; τ, fiber delay; FRM, Faraday rotator mirror; PD, photodiode; DAC, data acquisition card.

Based on the geometric approach of the β-separation line,[15] we estimate the linewidth at different observation time from the frequency noise PSD as follows:

$$\mathrm{FWHM} = (8\ln(2)A)^{1/2},$$

where A denotes the surface of the high modulation index area, which is the overall surface under the portion of $S_{\Delta\nu}(f)$ that exceeds the β-separation line $8\ln(2)f/\pi^2$. The expression is

$$A = \int_{1/T_0}^{f_c} H(S_{\Delta\nu}(f) - 8\ln(2)f/\pi^2)S_{\Delta\nu}(f)\mathrm{d}f,$$

where $H(x)$ denotes the Heaviside unit step function ($H(x) = 1$ if $x \geq 0$ and $H(x) = 0$ if $x < 0$), f_c denotes the intersection frequency of the β-separation line and $S_{\Delta\nu}(f)$, and T denotes the measurement time which prevents the observation of low frequencies below $1/T$.

Then 780 nm-band-related components are specially fabricated for the purpose of improving the 120° phase difference interference performance. Before conducting the measurement, we first test the pass-through spectrum of the equipment as shown in Fig. 2. Specifically, an amplified spontaneous emission (ASE) source is used as the input and the corresponding three-output spectrum measured by an optical spectrum analyzer is shown in Fig. 2. The results indicate that the laser wherein the frequency ranges from 728 nm to 980 nm is well detected by the measurement system and the testable range is limited by the bandwidth of the optical fiber components used. The measurement accordance within the whole range can be maintained by calibrating the instrument constants for different wavelengths. And the splitting ratio of the 3×3 coupler is almost 1 : 1 : 1, and the extinction ratios of the three interference fringes are 121, 106, 110. All the parameters are good to ensure that the instrument works properly.

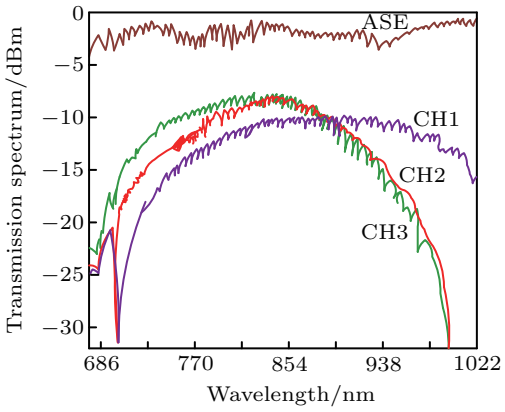


Fig. 2. The pass-through spectrum of the measurement system.

3. Experimental results and discussion

We investigate an integrated commercial semiconductor laser produced by Sacher Lasertechnik (Micron series lasers). The laser is a narrow-linewidth external-cavity semiconductor laser wherein the grating and shaping prism are solidified in the package to achieve miniaturized packaging and stable mechanical performance. However, it is not possible to change a few settings of the laser in such a structure. We operate the laser at 24.54 ℃ and 120 mA. Subsequently, the corresponding wavelength is 780.24 nm, the side mode suppression ratio exceeds 45 dB, and the output power is 10 dBm after it is coupled to a fiber patch cord through a series of space lenses under the frequency-locking condition. The output light is maintained at 10 dBm and is connected to the measurement system without any attenuation and then to the frequency fluctuation PSD of the laser. Thus, the linewidth at different integration time is obtained by introducing the β-separation algorithm as shown in Fig. 3. For example, the linewidth is about 2.8 MHz@100 ms, and 0.7 MHz@10 μs, which is larger than the value in the datasheet for worse pumping conditions and work status settings.[16] The integration time denotes the reciprocal of the corresponding frequency. As shown in the measured results, the integration-time linewidth slightly reduces within the frequency-locked bandwidth although it significantly decreases as the test time decreases when the integration frequency exceeds the bandwidth. The linewidth is almost the same at the frequency lower than 1 kHz because the peaks around 1 kHz possess most of the energy that causes the broaden of the linewidth. Additionally, the minimum linewidth is approximately 0.1 MHz, which corresponds to the point of the intersection between the β-separation line and the frequency fluctuation PSD line. The spikes at 750 Hz and their harmonics are introduced by the frequency-locked circuit, and the high-frequency spurs are due to the temperature control circuit. The grey line in Fig. 3 represents the frequency fluctuation PSD background of the measurement equipment, and the value is 1 Hz^2/Hz when considering the frequency band exceeding 10 kHz.

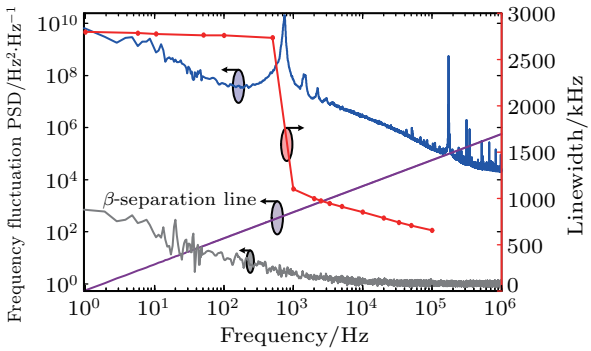


Fig. 3. The measured frequency fluctuation PSD and linewidth at different integration time. The blue line denotes the frequency fluctuation PSD; purple line, β-separation line; grey line, background frequency fluctuation PSD; and red dots, linewidth at different integration time. The blue, purple, and grey lines correspond to the left axis while the red line to the right axis.

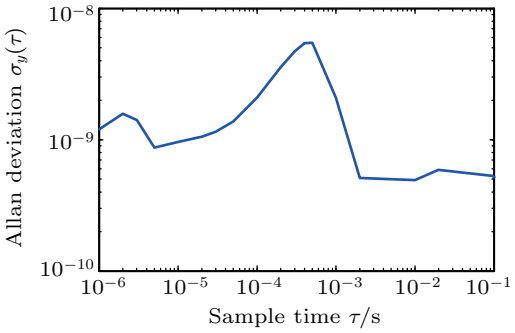


Fig. 4. The Allan deviation calculated from frequency fluctuation PSD.

Figure 4 shows the Allan deviation of the laser calculated from the frequency fluctuation PSD. The values are about 5.2×10^{-9}@100 ms, 2.1×10^{-9}@1 ms, and 1.2×10^{-9}@1 μs. The sharp peak in the laser frequency noise PSD at the frequency of 750 Hz and its harmonics significantly degrade the Allan deviation. The parameter is extremely important in characterizing the stability in the time domain of frequency signals in the optical domain and the radio-frequency domain and is widely used in several applications such as time and frequency transfer[17,18] and atomic clock.[19] Furthermore, it could be extended to measure the long-term stability of lasers provided that the interferometer is free from outside disturbances.

We change the pump current of the laser in steps of 10 mA to examine the relationship between the phase-frequency noise characteristics and pump current, as shown in Fig. 5. Eventually, we measure the frequency fluctuation PSD at currents of 90 mA, 100 mA, 110 mA, 120 mA, and 130 mA and the corresponding optical powers are 6.5 mW, 8.0 mW, 9.5 mW, 11.0 mW, and 12.5 mW, respectively. The driving temperature is maintained at 24.54 ℃ during the process. In this case, we investigate the phase-frequency characteristics under the condition of free running because it is difficult to adjust the pump current when the laser is frequency-locked. To eliminate the effects of instrument response at different power levels, we adjust the optical attenuator to maintain the incident light at 6.5 mW. The test results indicate that when the frequency is below 200 Hz, the laser under test and the measurement system are more susceptible to disturbances from the external environment. This implies that it is more difficult to eliminate the effects of vibration and sound. Therefore, the measured frequency fluctuation PSD of the laser shows a feature of randomness. In the frequency range of 200 Hz–300 kHz, the PSD increases with increasing pump current, and this is caused by the thermal effect. In particular, the operating temperature of the laser increases when the pump current increases, causing an increase in the flicker noise of the laser at low frequencies. However, when the frequency exceeds 300 kHz, the PSD decreases when the pump current increases because the laser is about to enter the white noise regime based on the Schawlow–Townes–Henry theory (the Gaussian white frequency noise level is inversely proportional to the laser power).

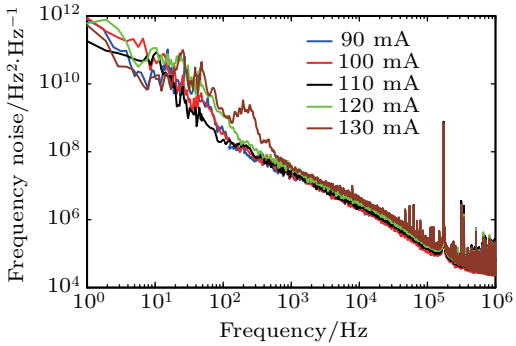


Fig. 5. The frequency fluctuation PSD at different pump currents.

We readjust the pump current to 120 mA and continue to investigate the phase-frequency noise characteristics of the laser before and after frequency lock by locking the laser to the D2 line of a saturated Rb absorption cell as shown in Fig. 6. The results indicate that the frequency fluctuation PSD of the laser is significantly suppressed in the frequency band below the frequency-locked bandwidth $B_{\rm w}$ (750 Hz) and subsequently gradually reverts to the state of free running when the frequency exceeds $B_{\rm w}$. The frequency fluctuation PSD at the state of frequency locking exceeds that of free running in the frequency band around $B_{\rm w}$ because the frequency-locked gain increases at the same time when the output power of the laser increases. Additionally, the spikes at the frequency of 750 Hz and their harmonics indicate that the locking condition is not adjusted to the optimal state. This is because the value potentially exceeds that of free running by an order of magnitude, and this is not a slight increase such as an ideal situation. We can evaluate and optimize the performance of the frequency-locked lasers based on the measured results.

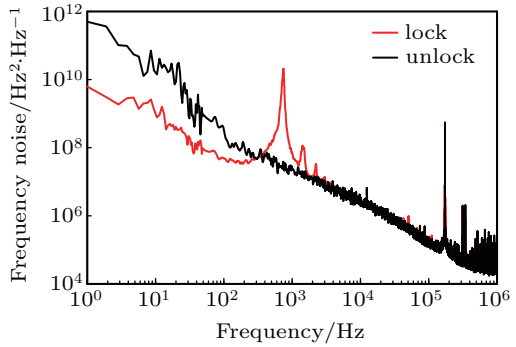


Fig. 6. The frequency fluctuation PSD before and after frequency locking.

In order to further examine the effects of the optimized frequency-locking loop on the phase-frequency noise characteristics of the lasers, we replace the laser under test with another commercial external cavity semiconductor laser produced by Toptica Photonics (DL100). We set the operating temperature at 25 ℃ and pump current at 150 mA. Subsequently, the output power of the optical fiber is 30 mW through

a series of space lenses. We measure the frequency fluctuation PSD under the conditions of free running and frequency lock. Additionally, we apply a modulation frequency on the laser, and the selected value is 200 kHz and 111 kHz as shown in Fig. 7. The results indicate that the applied modulation signal does not change the phase-frequency noise characteristics of the laser in the low frequency band while spikes appear at the corresponding modulation frequency and harmonics. The changes in the corresponding spikes are evidently observed from the measured results, and the frequency fluctuation PSD slightly changes when we change the modulation frequency. This is used to optimize the system and select a more suitable modulation frequency. The frequency PSD of the laser is significantly suppressed below the frequency-locked bandwidth $B_{\rm w}$ (2 kHz), this is consistent with the case when it is free running and the frequency exceeds $B_{\rm w}$, just like the analysis in Fig. 6. Nevertheless, the results indicate that the peak around $B_{\rm w}$ is extremely low, thereby indicating that the laser is in a stable frequency-locked state with optimum parameters. Additionally, the frequency fluctuation PSD of the laser in the frequency band below 10 Hz slightly exceeds that when the frequency exceeds 10 Hz, and this is caused by sudden changes in the frequency of the frequency-locked loop at the beginning.

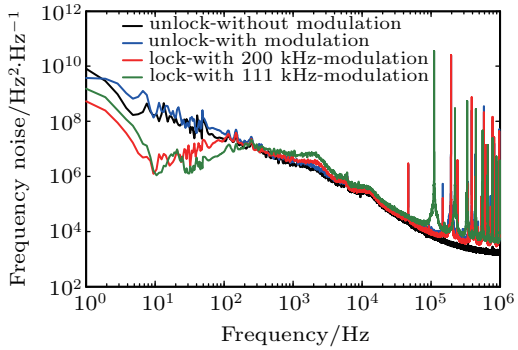


Fig. 7. The frequency fluctuation PSD before and after frequency locking and modulation.

4. Conclusion and perspectives

Based on a 120° phase difference interferometer, we proposed a short-delay homodyne interference method to directly test the phase-related parameters of single-frequency lasers in the 780 nm band commonly used in cold atomic clocks. We obtained the differential phase information of the laser by demodulating the three-way interference signals of the interferometer and subsequently calculated other parameters including differential phase noise PSD, phase noise PSD, single-band phase noise PSD, differential frequency noise PSD, frequency noise PSD, linewidth at different integration time, and Allan deviation based on the relationship between them. The pass-through spectrum of the measurement system ranged from 728 nm to 980 nm and could be expanded via specially designed fiber devices. Additionally, the measurement noise floor was approximately 1 $\rm Hz^2/Hz$ when the frequency exceeded 10 kHz and could be further improved by reducing the thermal noise of the system. Examples include using an integrated fiber system structure as opposed to discrete optical components; using a photonic crystal fiber instead of a traditional single-mode fiber as the delay fiber; and optimizing the interferometer package to better resist the disturbances such as external environmental noise and specifically the acoustic noise, vibration noise, and thermal noise. Subsequently, it could be used in more applications that require laser sources with ultra-low phase noise. Additionally, the testable frequency range increased via utilizing interferometer with higher FSR and suitable acquisition parameters.

Several phase-frequency noise characteristics of two commercial semiconductor 780 nm lasers used in integrating sphere cold atomic clocks were directly measured. Firstly, the linewidth increased with the increase of the integration time. Furthermore, spikes in the frequency fluctuation PSD significantly degraded the Allan deviation. Secondly, the phase-frequency noise of the laser in the low-band ($<$ 300 kHz) increased with the pump current, and this was potentially due to the thermal effects caused by the increase in current. While considering the frequency range from 300 kHz to 1 MHz, the frequency noise PSD decreased with increase in the current due to the decrease in the white noise component based on the Schawlow–Townes–Henry theory. Thirdly, when a saturated Rb absorption cell was used to stabilize the laser frequency, the locking parameters significantly affected the noise performance. The frequency fluctuation PSD was significantly suppressed when the frequency was lower than $B_{\rm w}$ and subsequently returned to the level of free running. The value around $B_{\rm w}$ slightly increased if the optimal frequency-locking parameters were set. Conversely, it corresponded to high oscillating spikes. Fourthly, when a modulation frequency was applied to the laser, it did not affect the frequency fluctuation PSD at most frequency bands apart from the corresponding frequency and its harmonics. At the modulation frequency, new spikes appeared and the values around the frequencies increased.

The measurement method and the obtained phase-related noise characteristics could be applied for the development, optimization, and characterization of lasers, the selection of laser sources used in specific applications, and helping the evaluation of atomic clock system performance.

References

[1] Duan Y X, Wang B, Xiang J F, Liu Q, Qu Q Z, Lu D S and Liu L 2017 *Chin. Phys. Lett.* **34** 073201

[2] Koenning T, Irwin D, Stapleton D, Pandey R, Guiney T and Patterson S 2014 *Conference on High Energy/Average Power Lasers and Intense Beam Applications VII*, 2–4 February 2014 San Francisco, CA, United States, p. 89620F

[3] Xiang J F, Cheng H N, Peng X K, Wang X W, Ren W, Ji J W, Liu K K, Zhao J B, Li L, Qu Q Z, Li T, Wang B, Ye M F, Zhao X, Yao Y Y, Lu D S and Liu L 2018 *Chin. Phys. B* **27** 073701

[4] Wang X M, Meng Y L, Wang Y N, Wan J Y, Yu M Y, Wang X, Xiao L, Li T, Cheng H D and Liu L 2017 *Chin. Phys. Lett.* **34** 063702

[5] Klehr A, Wenzel H, Brox O, Bugge F, Erbert G, Nguyen T P and Tränkle G 2009 *Conference on Novel in-Plane Semiconductor Lasers VIII*, 26–29 January 2009 San Jose, CA, United States, p. 72301I

[6] Lienhart F, Boussen S, Carraz O, Zahzam N, Bidel Y and Bresson A J A P B 2007 *Appl. Phys. B* **89** 177

[7] Carraz O, Lienhart F, Charrière R, Cadoret M, Zahzam N, Bidel Y and Bresson A J A P B 2009 *Appl. Phys. B.* **97** 405

[8] Sortais Y, Bize S, Nicolas C, Clairon A, Salomon C and Williams C 2000 *Phys. Rev. Lett.* **85** 3117

[9] Delehaye M, Millo J, Bourgeois P, Groult L, Boudot R, Rubiola E, Bigler E, Kersalé Y and Lacroûte C 2017 *IEEE Photonic. Tech. Lett.* **29** 1639

[10] Nguyen T, Klehr A, Brox O, Erbert G and Trankle G 2007 *CLEO/Europe - IQEC 2007 European Conference on Lasers and Electro-Optics and the International Quantum Electronics Conference,* 17–22 June 2007 Munich, Germany, p. 193

[11] Xu D, Yang F, Chen D J, Wei F, Cai H W, Fang Z J and Qu R H 2015 *Opt. Express* **23** 22386

[12] Nguyen T, Klehr A, Brox O, Erbert G and Trankle G 2009 *2009 Conference on Lasers & Electro-Optics Europe & 11th European Quantum Electronics Conference (CLEO/EQEC)*, 14–19 June 2009, Munich, Germany, p. 1

[13] Gruet F, Bandi T, Mileti G, Phelan R, O'Carroll J, Kelly B and O'Gorman J 2011 *2011 Conference on Lasers and Electro-Optics Europe and 12th European Quantum Electronics Conference (CLEO EUROPE/EQEC)*, 22–26 May 2011, Munich, Germany, p. 1

[14] Putra A W S, Yamada M, Ambran S and Maruyama T 2018 *IEEE Photonic. Tech. Lett.* **30** 756

[15] Barnes J A, Chi A R, Cutler L S, Healey D J, Leeson D B, McGunigal T E, Mullen J A, Smith W L, Sydnor R L, Vessot R F C and Winkler G M R 1971 *IEEE T. Instrum. Meas.* **IM-20** 105

[16] Di Domenico G, Schilt S and Thomann P 2010 *Appl. Opt.* **49** 4801

[17] Tombez L, Schilt S, Di Francesco J, Führer T, Rein B, Walther T, Di Domenico G, Hofstetter D and Thomann P 2012 *Appl. Phys. B* **109** 407

[18] Foreman S M, Holman K W, Hudson D D, Jones D J, Ye J 2007 *Rev. Sci. Instrum.* **78** 021101

[19] Feng Z T, Yang F, Zhang X, Chen D J, Wei F, Cheng N, Sun Y G, Gui Y Z and Cai H W 2018 *Sci. Rep.* **8** 13135

[20] Liu L, Lü D S, Chen W B, Li T, Qu Q Z, Wang B, Li L, Ren W, Dong Z R, Zhao J B, Xia W B, Zhao X, Ji J W, Ye M F, Sun Y G, Yao Y Y, Song D, Liang Z G, Hu S J and Yu D H 2018 *Nat. Comm.* **9** 2760